Supporting information for "Assessment of long tubing in measuring atmospheric trace gases: applications on tall towers"

Xiao-Bing Li[1,2,#], Chunsheng Zhang[3,#], Aiming Liu[3], Bin Yuan[1,2,*], Honglong Yang[3], Chanfang Liu[4], Sihang Wang[1,2], Yibo Huangfu[1,2], Jipeng Qi[1,2], Zhijie Liu[1,2], Xianjun He[1,2], Xin Song[1,2], Yubin Chen[1,2], Yuwen Peng[1,2], Xiaoxiao Zhang[1,2], E Zheng[1,2], Lei Yang[1,2], Qing Yang[1,2], Guangzhi Qin[1,2], Jun Zhou[1,2], and Min Shao[1,2]

[1] Institute for Environmental and Climate Research, Jinan University, Guangzhou 511443, China

[2] Guangdong-Hongkong-Macau Joint Laboratory of Collaborative Innovation for Environmental Quality, Guangzhou 511443, China

[3] Shenzhen National Climate Observatory, Shenzhen 518040, China

[4] Shenzhen Ecological and Environmental Monitoring Center of Guangdong Province, Shenzhen 518049, China

[#] Xiao-Bing Li and Chunsheng Zhang contributed equally.

[*] Corresponding author: byuan@jnu.edu.cn

Pressure drop and residence time of sample gas in tubing

The residence time of sample gas in a tubing could be theoretically calculated using Eq. (S1) as follows:

$$t = L\pi(d/2)^2/Q \tag{S1}$$

where t is residence time (s), L is the tubing length (cm), d is the inner diameter of the tubing (cm), Q is the flow rate of sample gas stream in tubing (cm^{-3} s^{-1}). In this study, the flow rate of the gas standard for various organic compounds was regulated by a mass flow controller (MFC) that was integrated into the PTR-ToF-MS. The PTR-ToF-MS can record changes in the flow rate of the gas standard. The residence time of sample gas stream in a tubing was defined as the difference of the time between the change in the flow rate of gas standard and the PTR-ToF-MS signal, as shown in Fig. S1. It should be noted that some auxiliary tubing with small diameters (e.g., 1/4" and 1/8") were used to connect different parts (e.g., PTR-ToF-MS, gas standard, and 1/2" tubes) of the measurement system. Therefore, the measured residence time of the sample gas in a 400 m-long tubing (OD: 1/2") at a flow rate of 13 SLPM is 155 s, which is slightly larger than that (131 s) calculated using Eq. (S1). The difference between the measured and calculated residence time may be mainly attributed to measurement errors for the tubing length and the flow rate, as well as the residence times caused by auxiliary tubes and associated parts of the instrument.

The pressure drop of the sample gas stream in a tubing could be estimated using the Hagen-Poiseuille equation as formulated in Eq. (S2-3). In addition to the change in pressure, the flow rate of sample gas in a tubing is also associated with changes in a set of other parameters. Therefore, the pressure of sample gas at the outlet end of the tubing can be theoretically estimated using Eq. (S3) when the pressure of sample gas at the inlet end of the tubing is known. Figure S2 shows the change of the pressure drop in response to a set of flow rates for a 400 m long PFA Teflon tubing (OD: 1/2"; OD: 0.374") when the pressure of sample gas at the tubing inlet is set as 1 atm (1000 hPa). It shows that the pressure drop of sample gas in the tubing rapidly increases with the increase in flow rate.

$$Pressure\ drop = (P_i - P_o)/P_i \tag{S2}$$

$$P_o = \sqrt{P_i^{\,2} - Q/(256\pi d^4 \eta L P_i)} \tag{S3}$$

where P_i is the pressure of sample gas at tubing inlet (hPa), P_o is the pressure of sample gas at tubing outlet, Q is the flow rate of sample gas stream in tubing (cm^{-3} s^{-1}), d is the inner diameter of the tubing (cm), η is the viscosity of sample gas in tubing (Pa s^{-1}), and L is tubing length (cm).

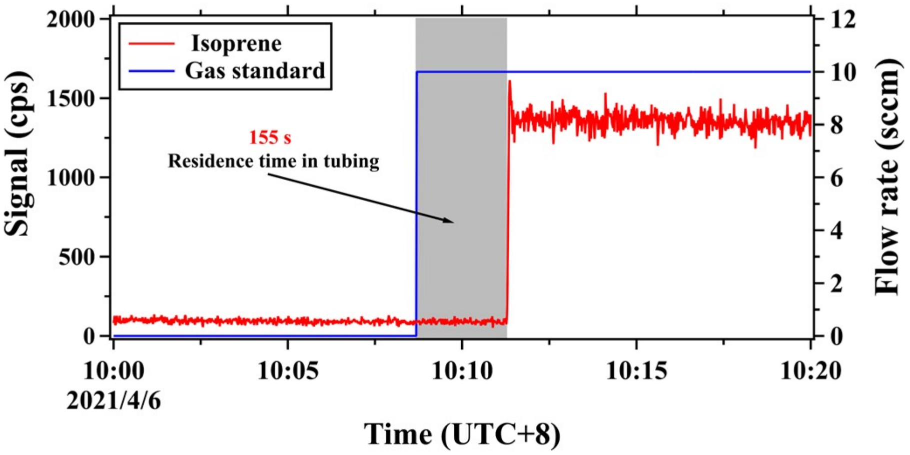

Figure S1. Time series of the PTR-ToF-MS signal of isoprene along with the change in the flow rate of the gas standard. The flow rate of the sample gas stream in the tubing is 13 SLPM.

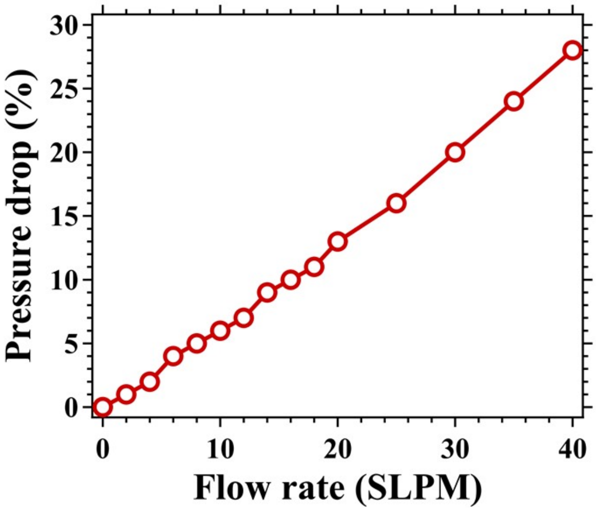

Figure S2. The change of pressure drop in response to a set of flow rates for a 400 m long PFA Teflon tubing (OD: 1/2"; ID: 0.374") when the pressure of sample gas at the tubing inlet is set as 1 atm.

Description of laboratory tests

As shown in Figure S3, the mixture of gas standard and zero air, was added to the tubing at a fixed flow rate. Flow rates of gas standard and zero air cylinders were regulated by two MFCs to ensure that the gas mixture has designated concentrations for various chemical species, namely organic compounds, NO, NO_2, and CO_2. A step-function change in concentrations of various gaseous species was realized by adjusting the flow rate of the gas standard. Concentrations of various chemical species were measured at both ends of the 400 m-long PFA Teflon tubing (Figures S4, S6, and S7) to quantitatively assess their measurement uncertainties after traversing the tubing. As shown in Figure S5, specific concentrations of ozone could be produced when passing zero air through an ozone generator. A step-function change in concentrations of ozone was realized by adjusting the intensity of the ultraviolet lamp in the ozone generator. In laboratory tests, concentrations of organic compounds (Tables S1-S2) were measured using PTR-ToF-MS. NO and NO_2 concentrations were measured using a NO_2/NO/NOx monitor (405, 2B Tech, USA). Ozone concentrations were measured using an ozone monitor (205, 2B Tech, USA). CO_2 mixing ratios were measured using the CO_2 and H_2O Gas Analyzer (Li-840A, Licor Inc., USA).

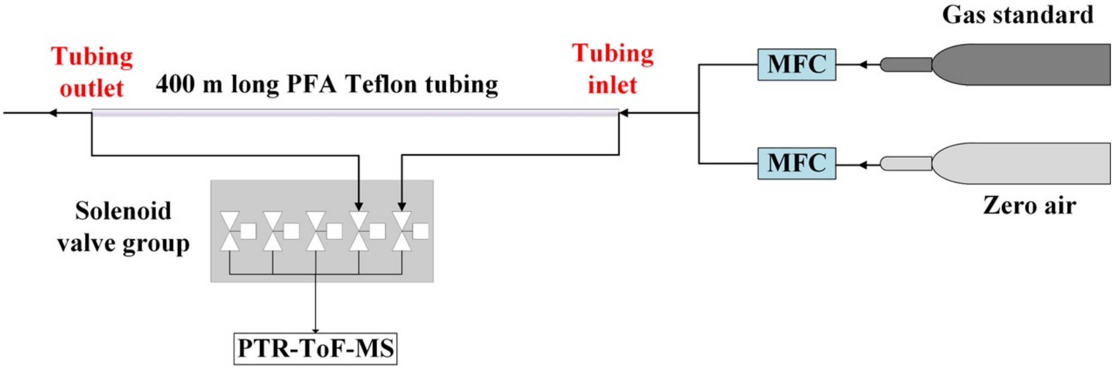

Figure S3. Schematic illustration of the PFA Teflon tubing test for NOx (NO and NO_2), CO_2, and various organic compounds.

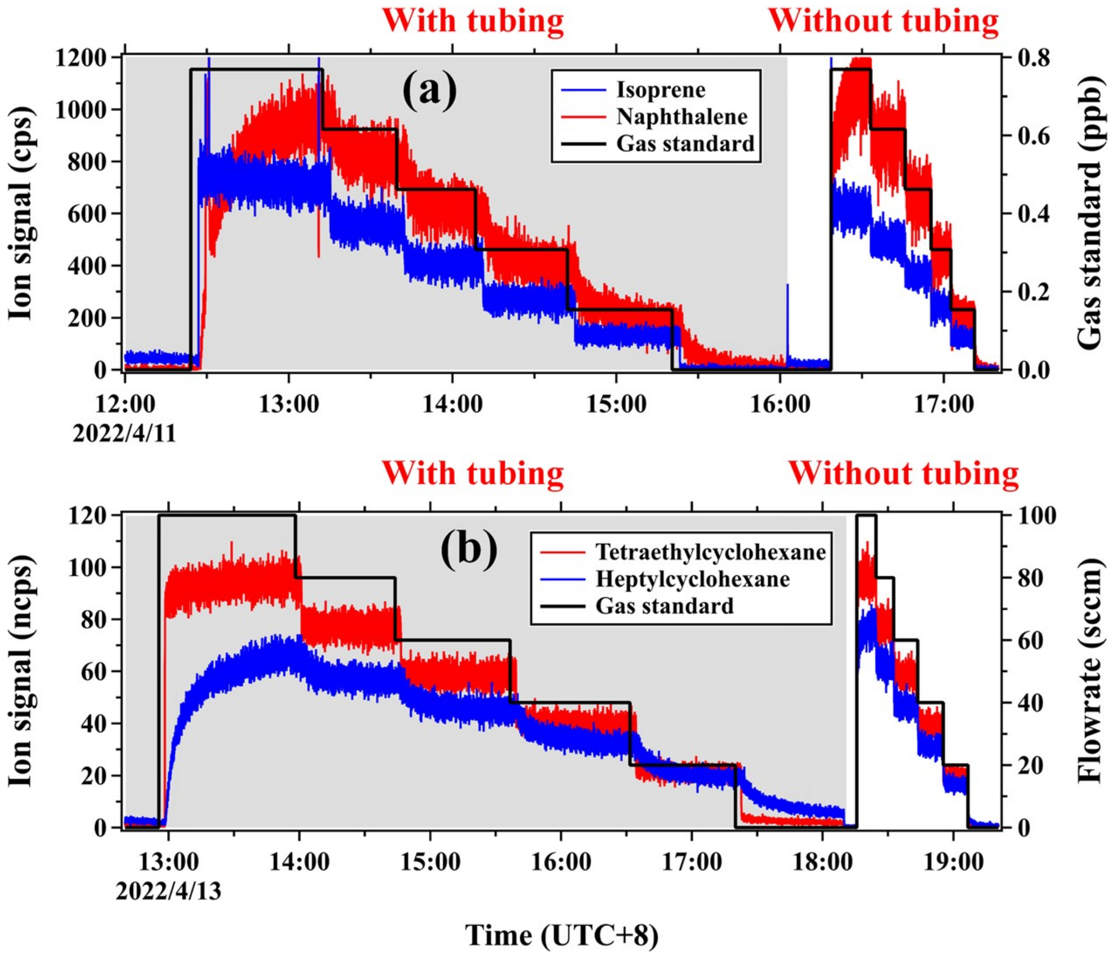

Figure S4. Time series of ion signals of two selected organic compounds in the gas standards measured by PTR-ToF-MS in (a) H_3O^+ mode and (b) NO^+ mode with and without the 400 m long PFA Teflon tubing, respectively. The flow rate of the sample gas stream in the tubing is 13 SLPM.

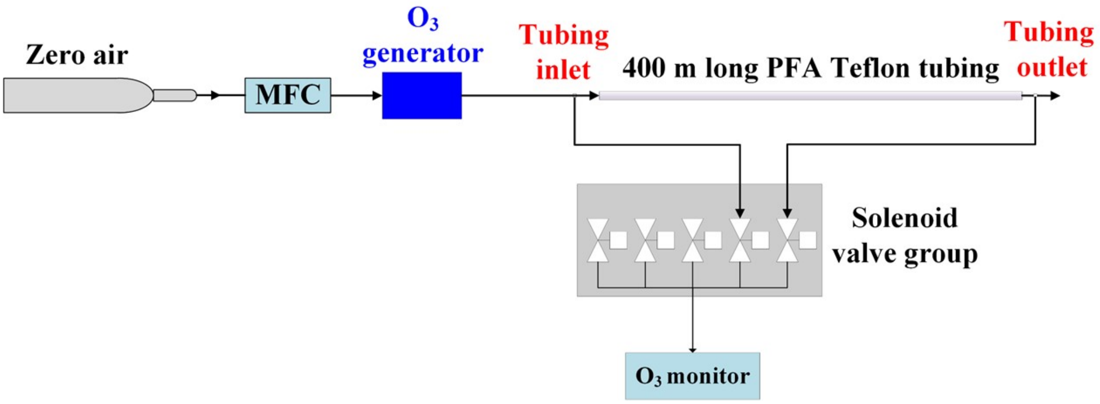

Figure S5. Schematic illustration of the PFA Teflon tubing test for ozone.

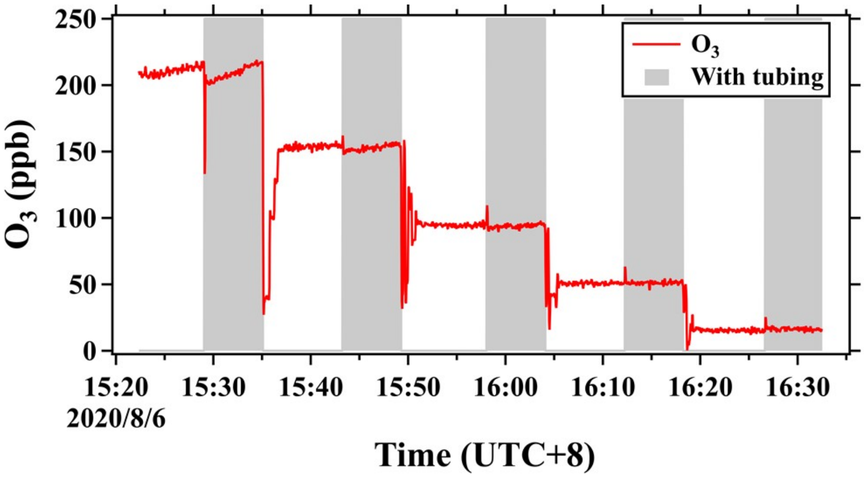

Figure S6. Time series of ozone mixing ratio measured with and without the 400 m long PFA Teflon tubing, respectively. The flow rate of the sample gas stream in the tubing is 8 SLPM.

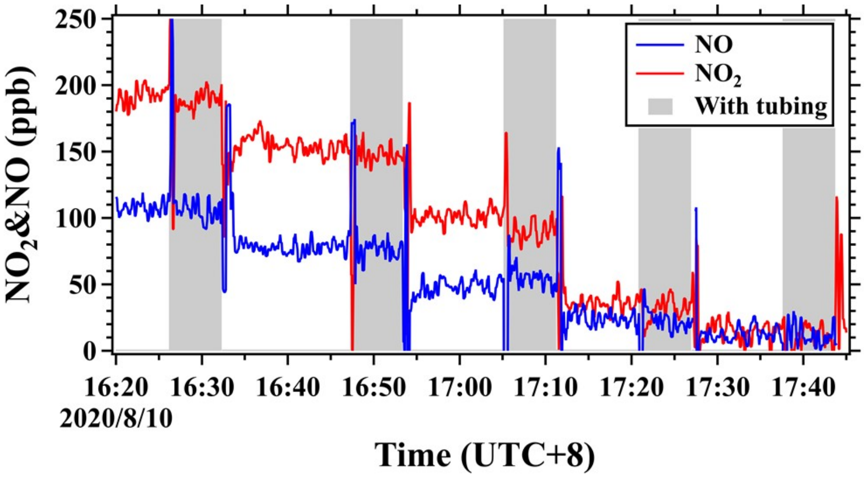

Figure S7. Time series of NO and NO_2 mixing ratio measured with and without the 400 m long PFA Teflon tubing, respectively. The flow rate of the sample gas stream in the tubing is 8 SLPM.

Table S1. Summary of the organic compounds in the gas standard measured by PTR-ToF-MS using H_3O^+ as ion source

No.	Species name	Chemical formula	m/z	C^* ($\times 10^6$, μg m^{-3}) ##
1	Hydrogen Cyanide	$HCNH^{\#}$	28	1074.6
2	Formaldehyde	$CH_2OH^{\#}$	31	1226.3
3	Methanol	$CH_4OH^{\#}$	33	456.1
4	Acetonitrile	C_2H_3NH	42	377.1

5	Acetaldehyde	C_2H_4OH	45	2281.3
6	Ethanol	$C_2H_6OH^\#$	47	205.3
7	Acrolein	C_3H_4OH	57	786.1
8	Acetone	C_3H_6OH	59	1085.6
9	Isopropyl alchol/2-Propanol/Isopropanol	$C_3H_8OH^\#$	61	261.4
10	Furan	C_4H_4OH	69	2212.7
11	Isoprene	C_5H_8H	69	2007.9
12	Methyl vinyl ketone	C_4H_6OH	71	308.7
13	2-Butanone/Methyl ethyl ketone	C_4H_8OH	73	2943.1
14	Hydroxyacetone	C_3H_6O2H	75	8.0
15	Benzene	C_6H_6H	79	423.7
16	2-Pentanone	$C_5H_{10}OH$	87	180.4
17	Ethyl Acetate	$C_4H_8O_2H$	89	530.1
18	Toluene	C_7H_8H	93	138.5
19	Phenol	C_6H_6OH	95	3.0
20	Furfural	$C_5H_4O_2H$	97	10.3
21	Methyl isobutyl ketone	$C_6H_{12}OH$	101	96.8
22	Styrene	C_8H_8H	105	33.6
23	o-Xylene	$C_8H_{10}H$	107	34.2
24	m-Cresol	C_7H_8OH	109	1.2
25	Chlorobenze	C_6H_5ClH	113	66.3
26	1,2,4-Trimethylbenzene	$C_9H_{12}H$	121	12.9
27	Guaiacol	$C_7H_8O_2H$	125	1.3
28	Naphthalene	$C_{10}H_8H$	129	1.4
29	α-Pinene	$C_{10}H_{16}H$	137	25.6
30	1,3-Dichlorobenzene	$C_6H_4Cl_2H$	147	9.4
31	Dodecane	$C_{12}H_{26}H^\#$	171	1.8
32	1,3,5-Trichlorobenzene	$C_6H_3Cl_3H$	181	2.9
33	D3 Siloxane	$C_6H_{18}O_3Si_3H$	223	138.5
34	D4 Siloxane	$C_8H_{24}O_4Si_4H$	297	25.5
35	D5 Siloxane	$C_{10}H_{30}O_5Si_5H$	371	6.0

[#] Tubing delays of these species were not obtained due to that their depassivation profiles were not well captured by PTR-ToF-MS.

[##] The saturated concentrations of organic compounds were calculated based on their saturated vapor pressure at 298 K obtained from the ChemSpider website (http://www.chemspider.com/).

Table S2. Summary of the organic compounds in the gas standard measured by PTR-ToF-MS using NO^+ as ion source

No.	Species name	Chemical formula	m/z	C* ($\times 10^6$, μg m^{-3}) [##]
1	Toluene	C_7H_8	92	138.5
2	Methacrolein	C_4H_4OH	69	535.7
3	Octane	$C_8H_{16}H$	113	87.1
4	Nonane	$C_9H_{18}H$	127	31.7
5	Decane	$C_{10}H_{20}H$	141	12.2
6	Undecane	$C_{11}H_{22}H$	155	5.0
7	Dodecane	$C_{12}H_{24}H$	169	1.8
8	Tridecane	$C_{13}H_{27}$	183	1.0
9	Tetradecane	$C_{14}H_{29}$	197	0.1
10	Pentadecane	$C_{15}H_{31}$[#]	211	0.1
11	Tetraethylcyclohexane	$C_{10}H_{18}H$	139	35.4
12	Pentylcyclohexane	$C_{11}H_{20}H$	153	3.3
13	Hexylcyclohexane	$C_{12}H_{22}H$	167	0.9
14	Heptylcyclohexane	$C_{13}H_{24}H$	181	0.1
15	Octylcyclohexane	$C_{14}H_{27}$	195	0.1

[#] The tubing delay of this species was not obtained due to that its depassivation profiles was not well captured by PTR-ToF-MS.

[##] The saturated concentrations of organic compounds were calculated based on their saturated vapor pressure at 298 K obtained from the ChemSpider website (http://www.chemspider.com/).

Tubing delays of organic compounds

According to the method used in the work by Karion et al., (2010), the influence times of molecular diffusion and dispersion, denoted by t_m (s), on measured concentrations of trace gases after traversing a tubing can be estimated using Eq. (S4),

$$t_m = X_{eff}/\bar{V} \tag{S4}$$

where $\bar{V}$ is the average flow velocity (cm s^{-1}) in tubing, X_{eff} is the effective distance (cm) of molecular dispersion, namely the longitudinal mixing length of molecules driven by molecular diffusion and Taylor dispersion; X_{eff} can be estimated using Eq. (S5),

$$X_{eff} = \sqrt{(2D_{eff}t)} \tag{S5}$$

where t (s) is the residence time of the air sample in tubing, D_{eff} is the effective molecular diffusion coefficient (cm^2 s^{-1}) and can be estimated using Eq. (S6),

$$D_{eff} = D + a^2\bar{V}^2/48D \tag{S6}$$

where D is the molecular diffusion coefficient (cm^2 s^{-1}) of the trace gas in air and a is the inner radius (cm) of the tubing.

The molecular diffusion coefficients of isoprene and chlorobenzene are ~0.085 and 0.075 cm^2 s^{-1}, respectively. The estimated t_m for isoprene and chlorobenzene when traversing the 400 m long tubing (a=0.475 cm) at different flow rates are summarized in Tables S3 and S4.

We can also assume a relatively large organic molecule (usually characterized by a small C^* value) with D=0.04 cm^2 s^{-1}, the t_m of which can be considered the maximum influence time of molecular diffusion and dispersion on measured concentrations of organic compounds after traversing the tubing. The t_m of the assumed species is estimated as 5.5 s at the flow rate of 13 SLPM and as 4.7 s at the flow rate of 18 SLPM after traversing the 400 m long tubing.

Table S3. Summary of the t_m and tubing delay for isoprene (C^*= 2.0×10^9 µg m^{-3}) after traversing the 400 m tubing at different flow rates

Flow rate	t_m (s)	tubing delay (s)
6.0	5.6	16.9
10.0	4.3	9.9
13.0	3.8	6.2
15.0	3.5	5.4
18.0	3.2	4.0

Table S4. Summary of the t_m and tubing delay for chlorobenzene (C^*= 6.6×10^7 µg m^{-3}) after traversing the 400 m tubing at different flow rates

Flow rate	t_m (s)	tubing delay (s)
6.0	6.0	289.7
10.0	4.6	154.6
13.0	4.0	100.1
15.0	3.8	47.5
18.0	3.4	44.6

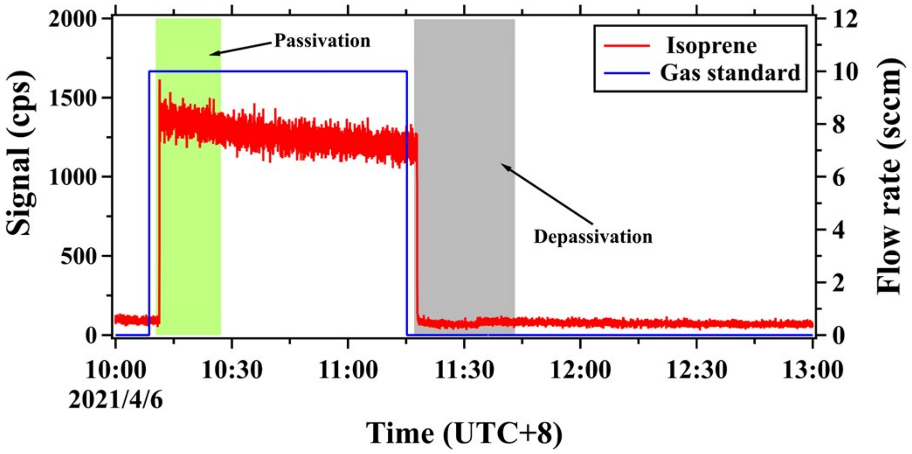

Figure S8. Time series of the PTR-ToF-MS signal of isoprene along with the change in the flow rate of gas standard. The flow rate of the sample gas stream in the tubing is

13 SLPM.

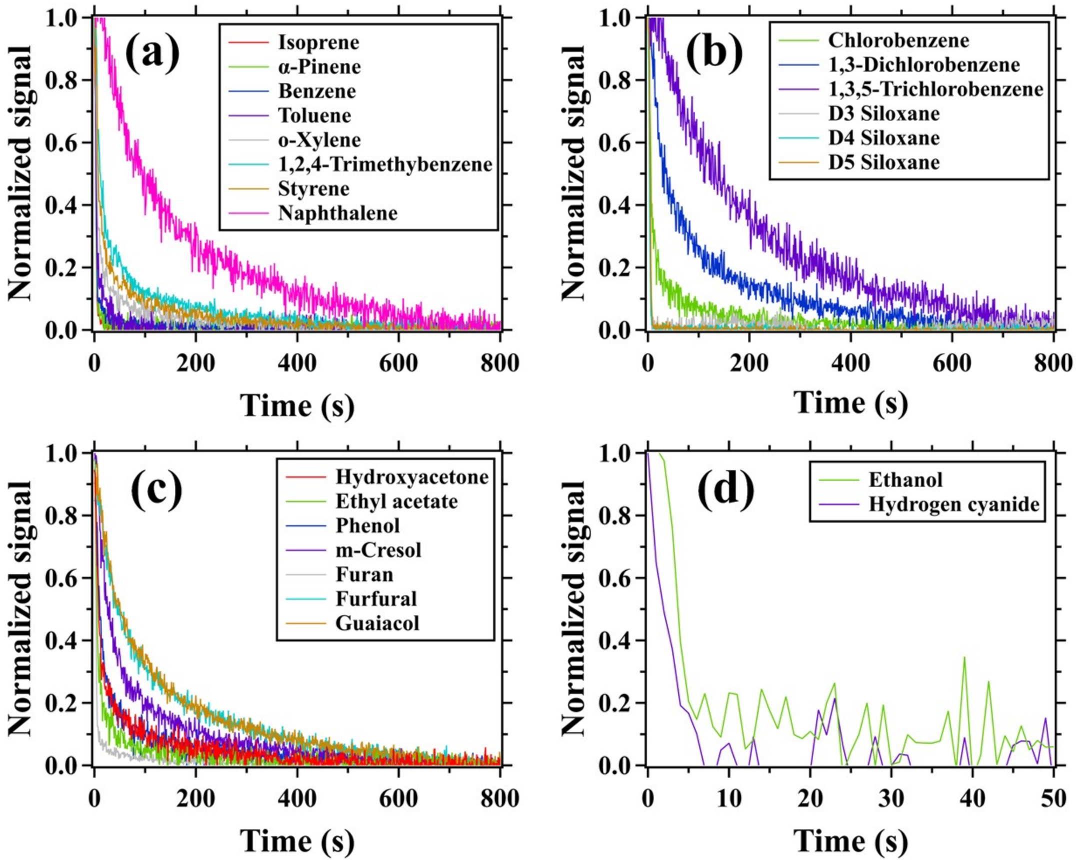

Figure S9. Time series of normalized PTR-ToF-MS signal using H_3O^+ as ion source in response to a step-function change in concentrations of various organic compounds measured at the outlet end of the 400 m long tubing with a flow rate of 13 SLPM.

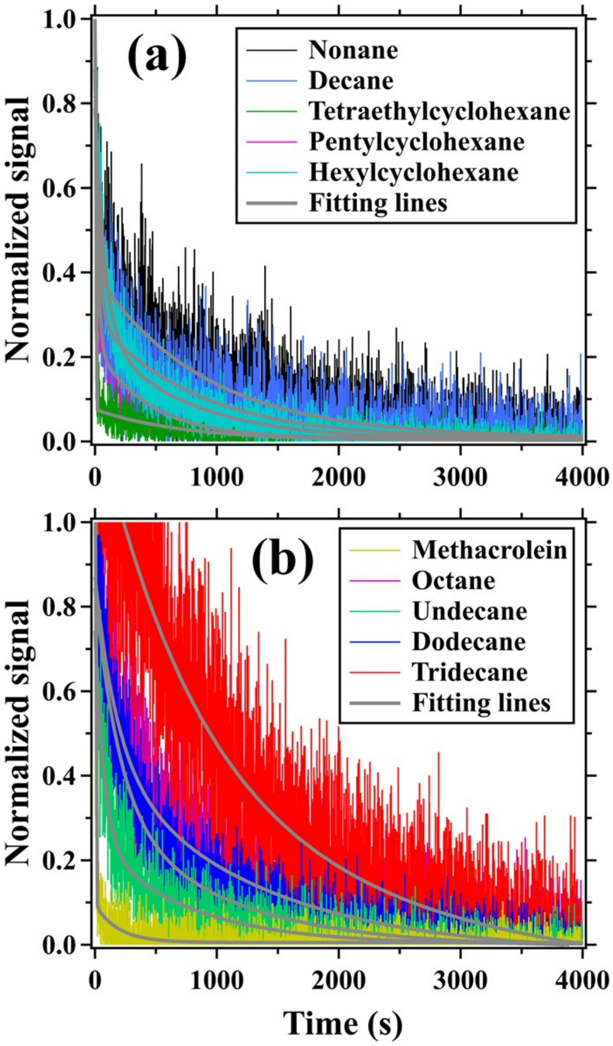

Figure S10. Time series of normalized PTR-ToF-MS signal using NO^+ as ion source in response to a step-function change in concentrations of various organic compounds measured at the outlet end of the 400 m long tubing with a flow rate of 13 SLPM.

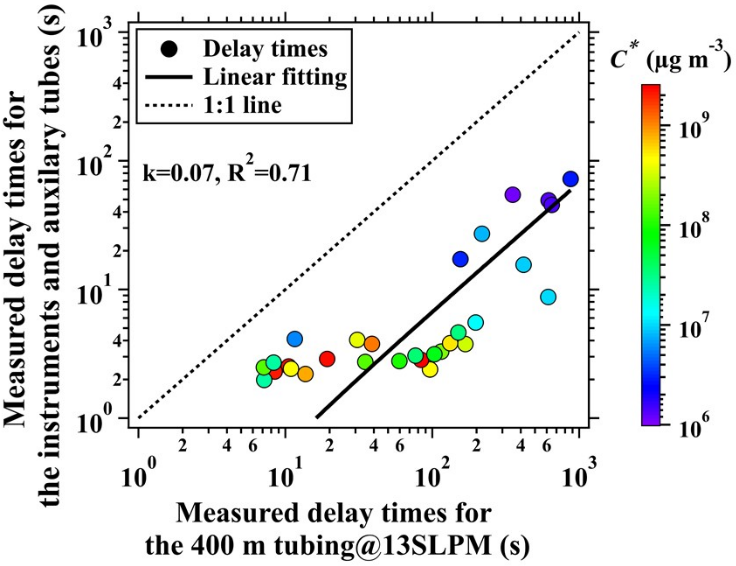

Figure S11. Scatter plots of the measured delay times for the instruments and auxiliary tubes versus those measured for the 400 m tubing at a flow rate of 13 SLPM.

Site description and field campaign

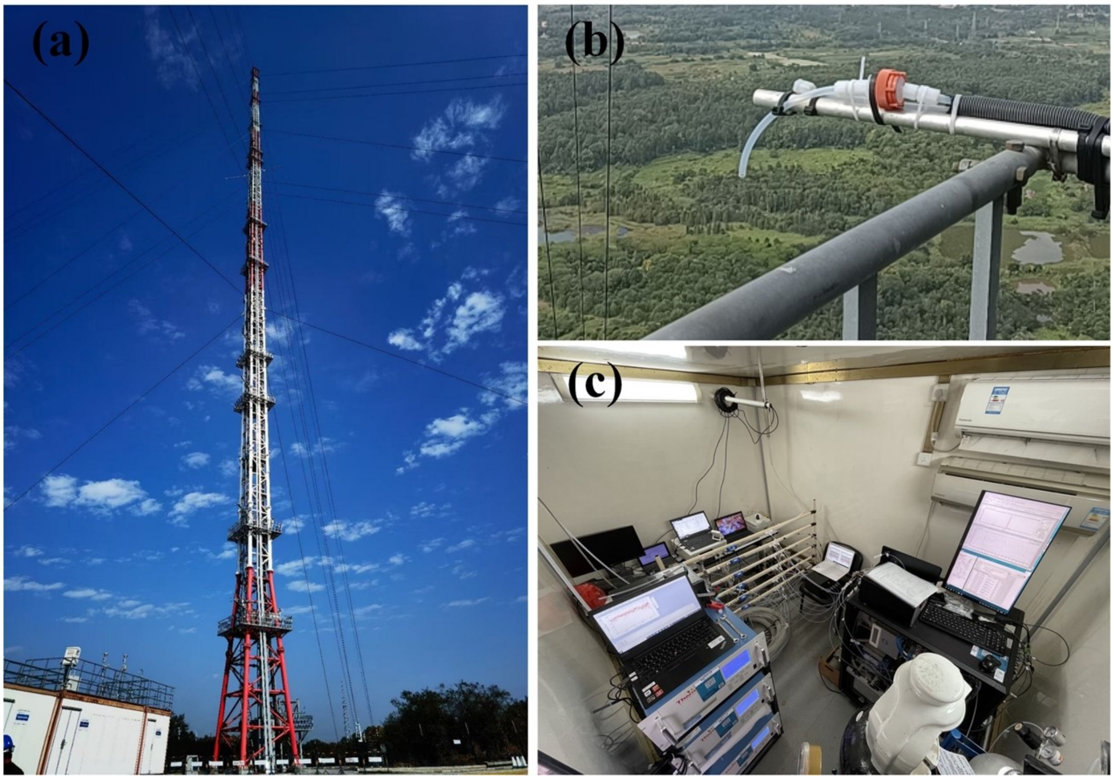

Figure S12. Pictures showing (a) the Shiyan Meteorology Tower (SMT), (b) the sampling inlet of the tubing on SMT, and (c) instruments in the observation room.

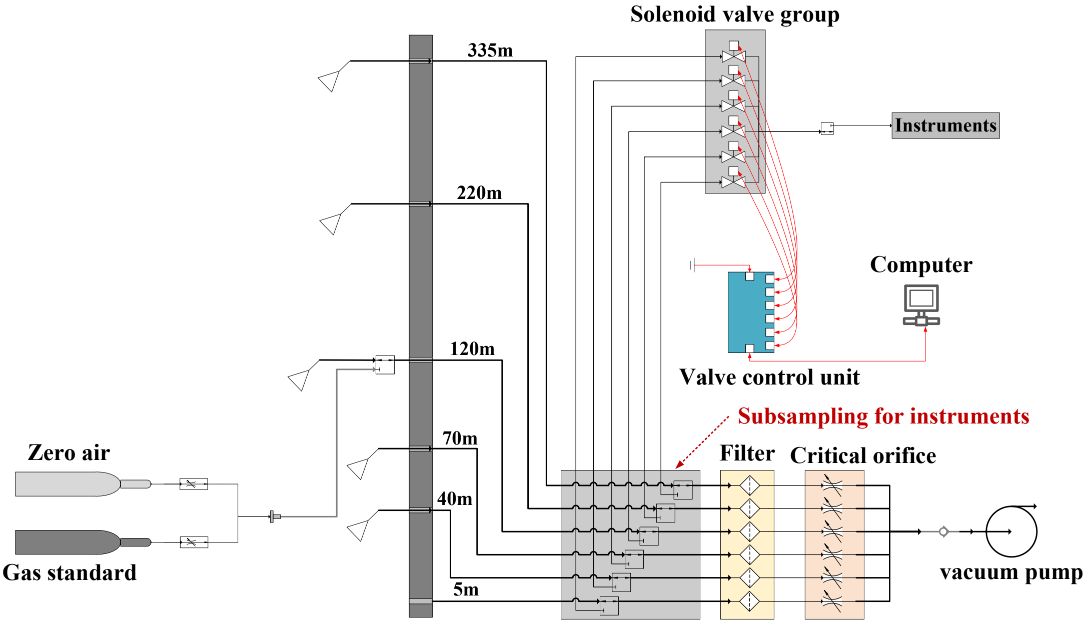

Figure S13. A simple schematic illustration of the vertical observation system on the SMT and locations of the six sampling inlets for measuring atmospheric gaseous species.

Table S5. Summary of tubing parameters for the six inlet heights

Inlet height (m)	**Tubing length (m)**	**Pressure* (kPa)**	**Flow rate$^{\#}$ (SLPM)**
5	5	93.4	14.75
40	120	87.1	13.83
70	150	89.7	13.86
120	200	90.6	13.35
220	300	86.2	13.76
335	400	84.6	12.56

* The pressure of air sample at the sub-sampling position.

$^{\#}$ The flow rate of air sample in tubing (OD: 1/2") without sub-sampling for instruments.

Box model simulation

Table S6. Summary of the box model settings

Parameters	Model settings
Time period	Illumination: 11:00:00-13:59:40 Dark: 14:00:00-14:30:00
Time step	20 s
Average pressure	1013.2 mBar
Average T	302.3 K
Average RH	47.4%
Emission intensity of Organic compounds	2 ppb
K dilution	0
Organic compounds	Isoprene, monoterpenes (α-pinene, 1ppb; β-pinene, 1ppb), Ethene, propene, 1-butene, n-pentane, Styrene, toluene
O_3	100/50 ppb
NO	5 ppb
NO_2	25 ppb
Background	0 ppb for all species

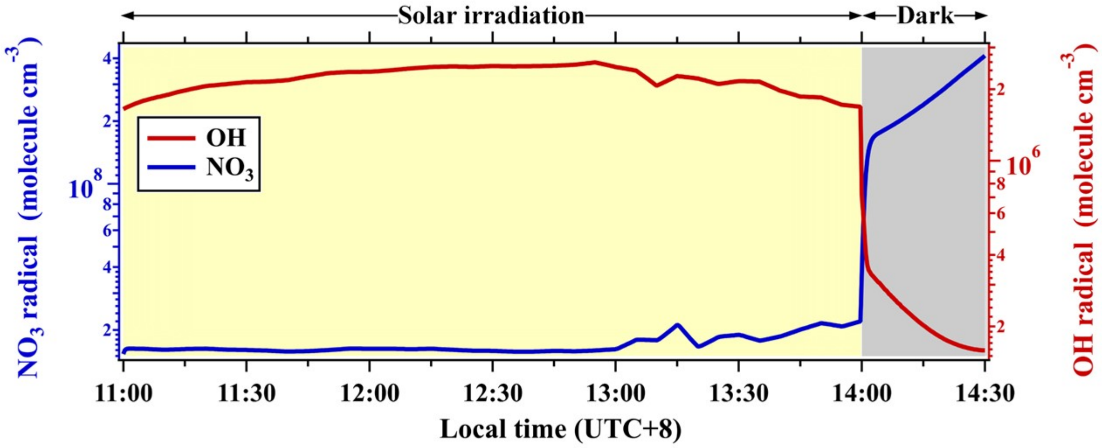

Figure S14. Time series of modelled NO_3 and OH radical concentrations in light and dark environments when the initial mixing ratio of ozone was set as 100 ppb.

Field validation results

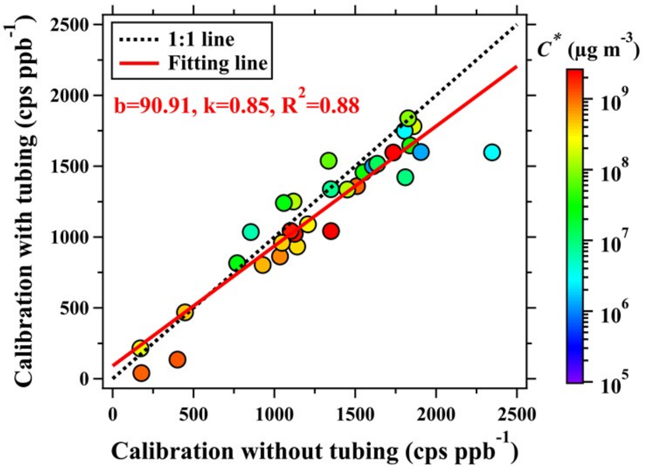

Figure S15. Intercomparison of species signals measured before and behind the 400 m long tubing (two 200 m long tubes for sampling air samples at 120 m on the SMT) at a flow rate of ~15 SLPM.

Box model results

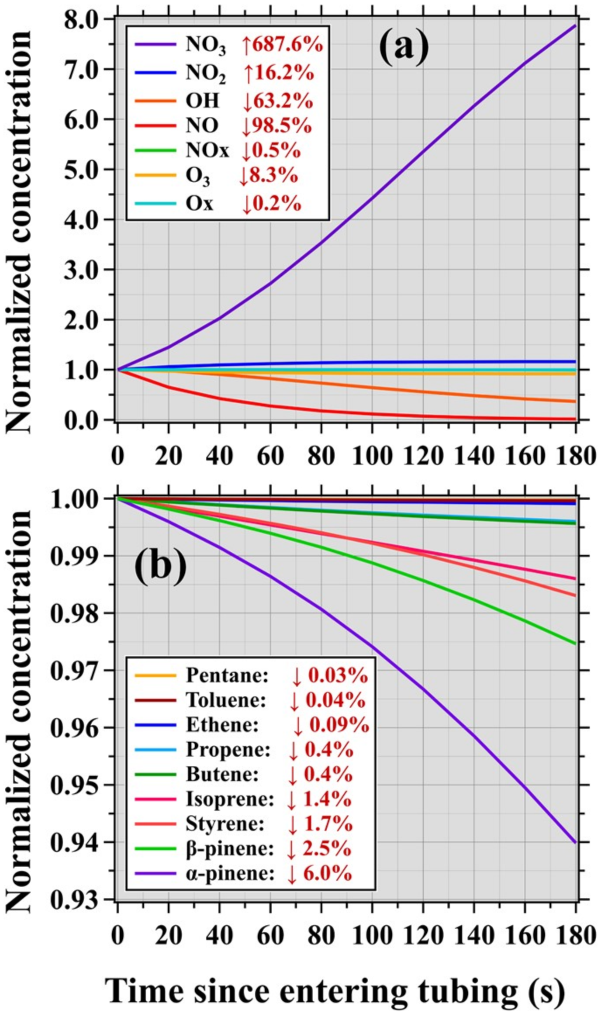

Figure S16. Time series of normalized concentrations of various chemical species since setting solar irradiation as zero (entering the tubing) in the box model when the initial mixing ratio of ozone was set as 50 ppb.

Field validation results

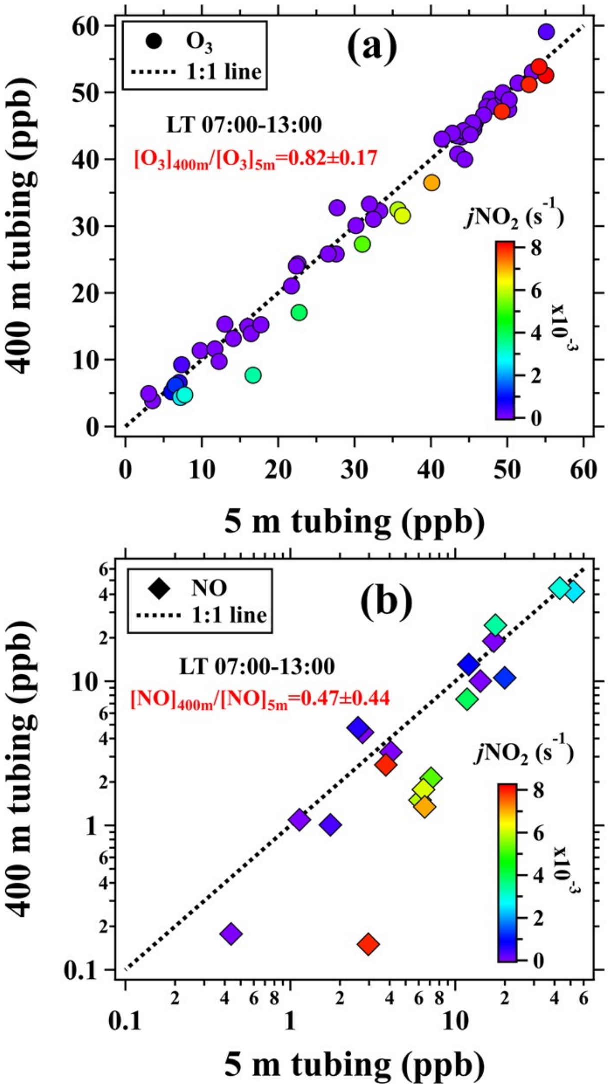

Figure S17. Intercomparisons of (a) ozone and (b) NO mixing ratios measured at ground level using a 400 m and a 5 m long tubing.

Tower observations

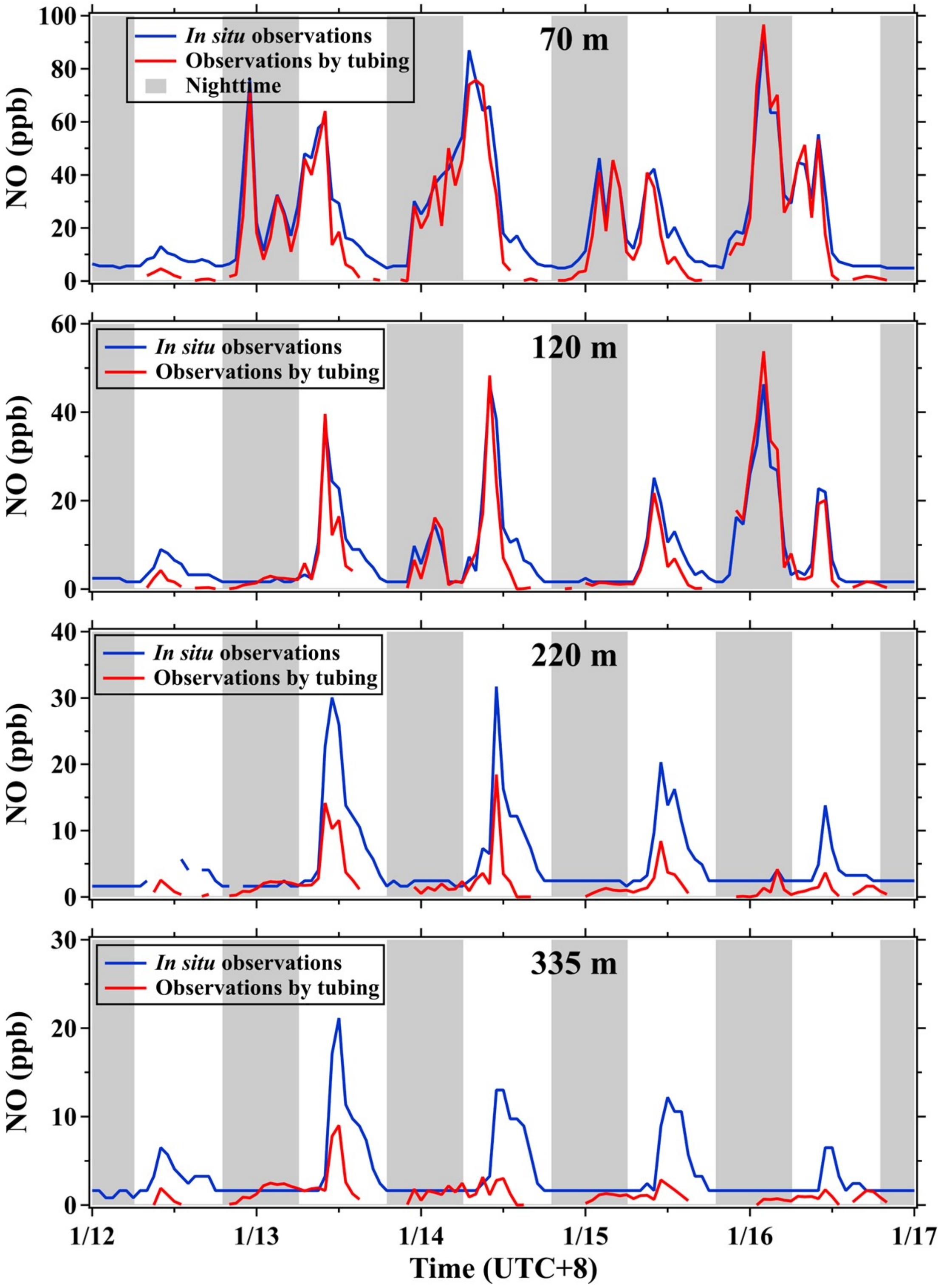

Figure S18. Time series of NO mixing ratios measured at the four altitudes on SMT from January 12 to 16, 2021. The grey areas indicate the nighttime period (LT 19:00-05:00).

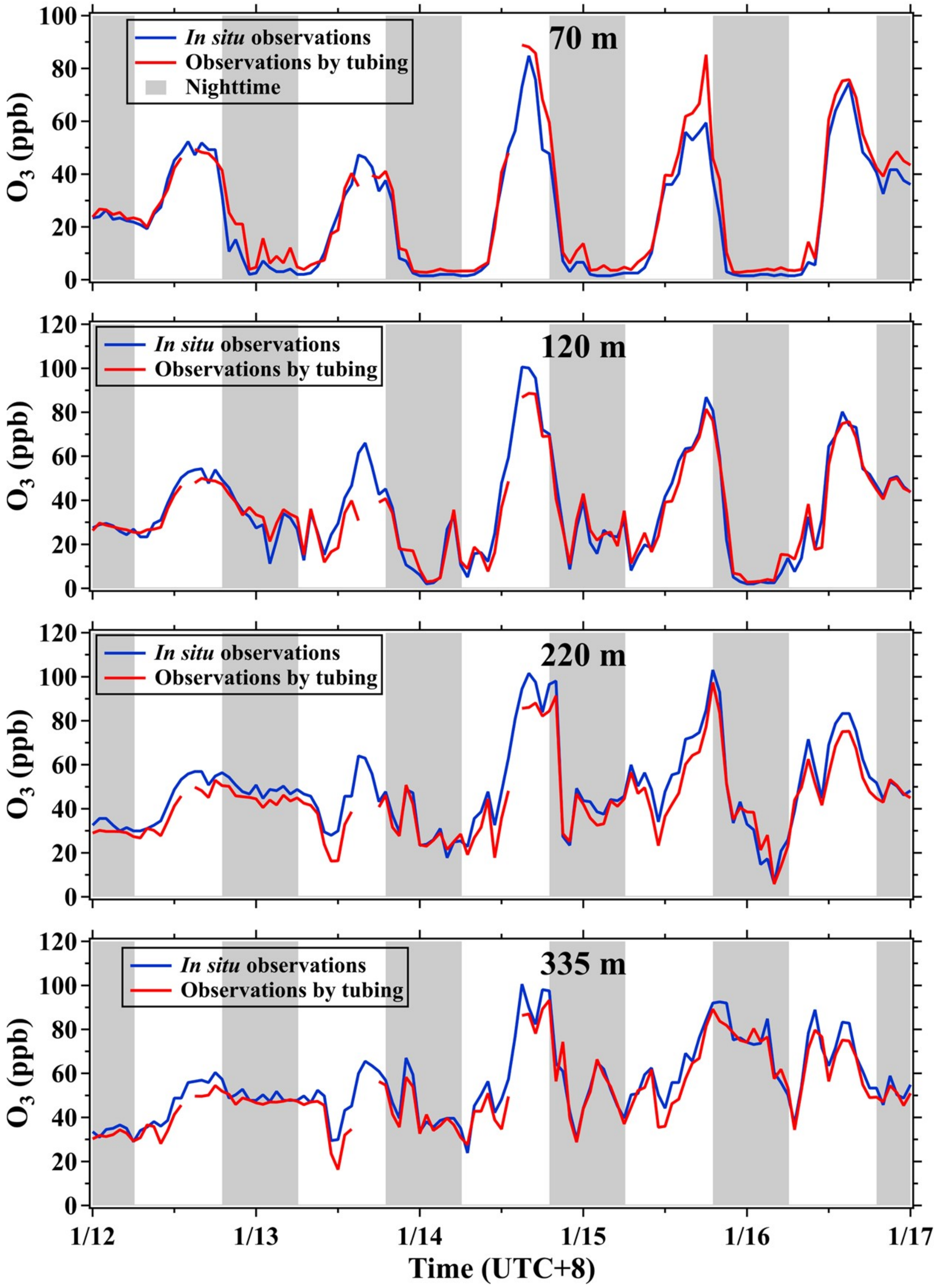

Figure S19. Time series of ozone mixing ratios measured at the four altitudes on SMT from January 12 to 16, 2021. The grey areas indicate the nighttime period (LT 19:00-05:00).

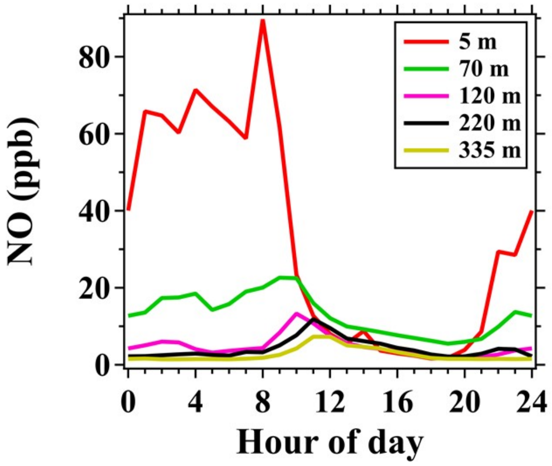

Figure S20. Average diurnal profiles of NO mixing ratios measured by different tower platforms (*in situ* observations) on SMT from January 8 to 26, 2021.

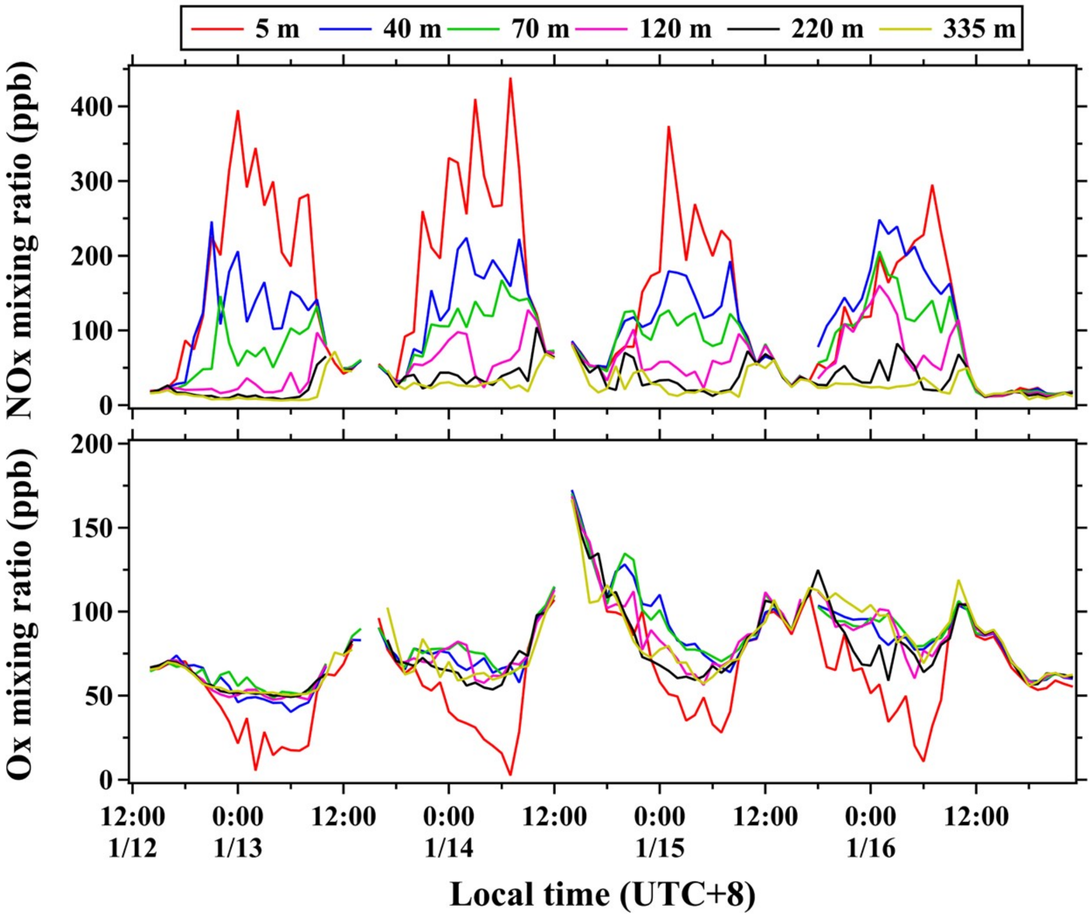

Figure S21. Time series of NOx and Ox mixing ratios at different heights measured by the vertical observation system.

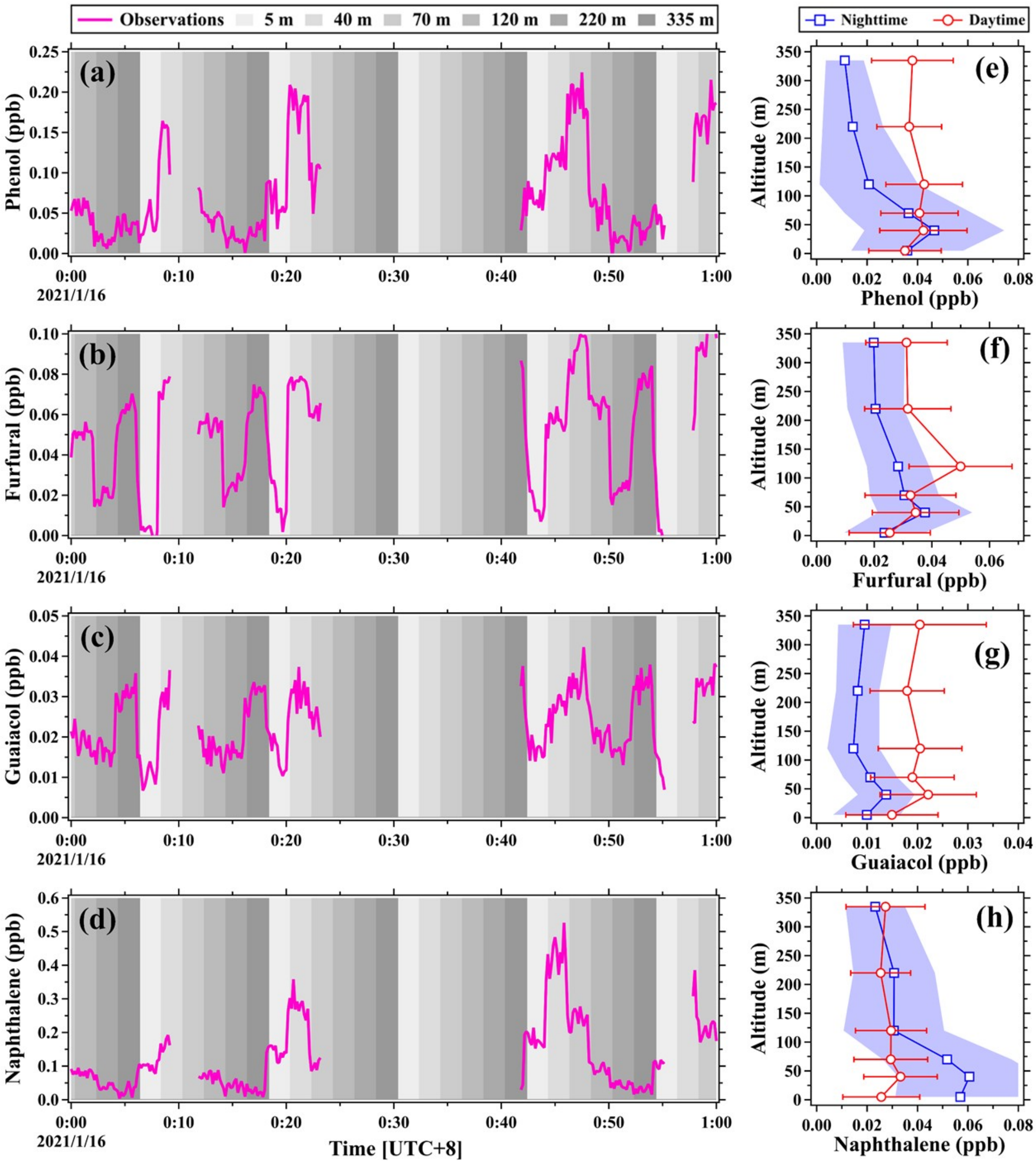

Figure S22. (a-d) Time series of mixing ratios of the selected chemical species with small values of *C** measured by the vertical observation system at the SMT site. (e-h) Mean vertical profiles of the selected chemical species (mean ± 0.5 standard deviations) for daytime (LT 10:00-16:00) and nighttime (LT 22:00-05:00) from January 16 to 29, 2021.